Jamming/flowing transition of non-Brownian particles suspended in a iso-density fluid flowing in a 2D rectangular duct

Maxym Burel, Sylvain Martin, Olivier Bonnefoy

EPJ Web of Conferences **140**, 03086 (2017) DOI: 10.1051/epjconf/201714003086
Powders & Grains 2017

Jamming/flowing transition of non-Brownian particles suspended in a iso-density fluid flowing in a 2D rectangular duct

Maxym Burel[1], *Sylvain* Martin[1], and *Olivier* Bonnefoy[1,⋆]

[1] *Ecole des Mines, SPIN, UMR CNRS LGF-5703, Saint-Etienne, F-42023 France*

Abstract. We present the results of an experimental study on the jamming/flowing transition. A suspension of neutrally buoyant large particles flows in an horizontal rectangular duct, where an artificial restriction triggers jamming. We show that the avalanche distribution size is exponential, that is memoryless. We further demonstrate that the avalanche size diverges when the restriction size approaches a critical value and that this divergence is well described by a power law. The parameters (critical opening size and divergence velocity) are compared to literature values and show a strong similarity with others systems. Another result of this paper is the study of the influence of the particle morphology. We show that, for a moderate restriction size, the dead-zone formed right upstream of the restriction is larger for angular particles but, paradoxically, that the avalanche size is larger for polyhedra compared to spheres by at least one order of magnitude.

1 Introduction

1.1 Context and objectives

Suspensions of solid particles in a fluid are of interest in many practical situations encountered in mining, polymer and oil/gas industries, just to name a few. The different models take into account a variety of interesting and challenging physical phenomena such as sedimentation/flotation, agglomeration, shear-thickening or shear-thinning. Most of these models rely on the assumption that the suspension is homogeneous (particles size very small compared to the flow length scales). In some contexts, however, solid particles may have a large diameter compared to the flow scales. For example, in the petroleum extraction industry, rock fragments suspended in oil may be, even individually, larger than the sediment pore throat. In the chemical industry, sticky polymer particles suspended in a liquid can form large agglomerates that are only one or two orders of magnitude smaller than the diameter of the transfer pipe. In this kind of situations, one may observe a clogging leading to a permeability decrease, a pressure loss increase or a pipe blockage. To reduce or mitigate the subsequent technical damages (pipeline erosion or failure), safety issues (fluid leakage) and economic losses (non-production costs), it is necessary to improve the understanding of such physical systems.

1.2 State-of-the-Art

In this section, we present a short survey of the literature dedicated to the transport of dense suspensions with a special care on the jamming event, which is the transition between the flowing and jammed states. More specifically, we will focus on flows involving 'large' particles, that is (1) the confinement effect is important: a discrete description prevails over a continuous description because the particle size is not much smaller than the system scale, and (2) the suspension is non-Brownian: the influence of the thermal fluctuations on the particles trajectory is negligible. As a consequence, particles are essentially driven by gravity, viscous drag and contact forces (particle-particle and particle-wall).

The jamming transition has been studied in several experimental conditions. The granular flows can be driven by viscous drag or gravity, in a cylindrical or rectangular pipe. Usually a restriction is located at the end (horizontal layout) or the bottom (vertical layout). Most authors count the number of grains flowing through the orifice between two jammed states (an avalanche) and perform a statistical analysis.

For gravity-driven flows of dry granular media, To [1] used a random walk model to predict the jamming probability. The model showed a good agreement with his experimental data. Zuriguel [2] and Garcimartin [3] results showed the independence between consecutive runs and found a geometric distribution for the jamming probability. For the same system, Janda [4] found that there is no critical size of restriction/orifice, which leads to the absence of jamming or, in other words, that every system can jam, whatever the restriction size. Gravity-driven flows of granular material immerged in a liquid have been tested by Wilson [5]. In contrast with dry granular material, he showed that the flowrate of the particles flowing through

⋆e-mail: olivier.bonnefoy@emse.fr

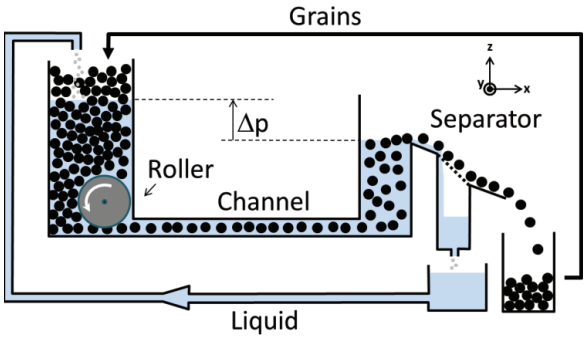

Figure 1. Side view of the experimental device.

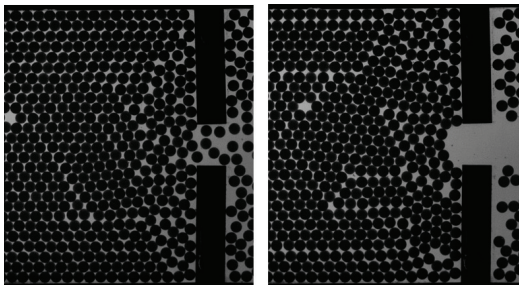

Figure 2. Snapshots of flowing vs. jammed suspension.

the orifice increases with the granular packing height. The underlying mechanism is not completely elucidated yet.

Viscous drag-driven particles flows have been investigated by Guariguata [6] and Lafond [7]. Guariguata studied the stationary flow of floating disks in an open channel and showed that the Beverloo law [8] is observed, and that the fluid velocity does not affect significantly the jamming probability. Lafond [7] used immerged polydisperse particles in an open channel and established a correlation between the jamming rate and the liquid flow rate.

For non-Brownian coarse particles suspensions, Vithal and Sharma [9] identified two jamming mechanisms: the sequential bridging and the multi-bridging.

In this study, we explore the behavior of a suspension of completely immerged particles subjected to a liquid viscous drag, without buoyancy effects, in a horizontal quasi-2D configuration. To our knowledge, this layout has not been studied before. More precisely, we want to address the following questions: (i) what is the influence of the liquid flowrate on the avalanche size ? (ii) is there a critical restriction size above which the system never jams ? and (iii) how is the jamming probability affected by non-spherical (non-cylindrical) particle morphology ?

2 Material and Method

2.1 Experimental set-up

The experimental setup is mainly composed of a feeder, a rectangular duct and a separator (figures 1 and 2). The **feeder** is a vertical recipient made of PMMA that contains particles. The porous space is filled with the suspending liquid in the lower half and with air in the upper half. A soft roller located at the bottom of the feeder entrains the particles into the horizontal rectangular duct, at a delivery rate controlled by its rotational speed. It is designed in order to distribute the particles evenly along the transverse y direction. The **rectangular duct** (length $L = 1200$ mm and width $W = 140$ mm is also made of transparent PMMA. The height H is chosen equal to 1.25 times the particle diameter such that only one layer of particles is allowed in the duct (quasi-2D). The channel cross-section area is $\Sigma_c \equiv W.H = 10.5$ cm^2. The suspension is forced to flow through a restriction of width w. The suspension flow is recorded by a camera at 200 fps with a resolution of 15 pixels by particle diameter. The **separator** is essentially composed of a sieve that removes the particles from the suspending liquid. The system operates in stationary conditions thanks to a pump.

2.2 Particles and liquid

The experiments are performed with a suspension of polyethylene particles. We use two sets of particles: spheres of 5.92 ± 0.02 mm diameter and polyhedral particles. The morphology is quantified by the departure to sphericity, as measured by the aspect ratio, equal to 1 for spheres and 0.75 ± 0.05 for polyhedra. In order to cancel buoyancy, we use a mixture of water and glycerol with the same density as solid particles (1050 ± 1 kg.m^{-3}). The fluid mixture is Newtonian, with a dynamic viscosity of 1.68 mPa.s. For all our experimental conditions, the suspension is non-Brownian (Peclet $> 10^{12}$) and discontinuous (Knudsen between 0.05 and 0.5).

2.3 Operating protocol

Initially, the feeder is filled with particles and liquid in its lower half, and the horizontal channel is filled with liquid at rest. A typical experimental run is composed of the following steps: (1) The roller is turned on at 200 rpm. This creates a dense 2D granular packing that is pushed towards the restriction until the system jams (arch formation). Then, the roller is stopped. (2) The peristaltic pump is turned on, with a rotational speed chosen to impose a given flowrate. Around 5 seconds are needed for the system to be stationary. (3) The horizontal duct is gently tapped to break the arch and start the discharge flow. (4) After some time, the system naturally jams again by forming a stable arch of particles. (5) The two previous steps are repeated 350 times to give robust statistics.

3 Results

Fig. 2 shows two typical top views. On the left, the particles are flowing through the restriction entrained by the viscous fluid. On the right, the system is jammed and a stable arch is clearly visible at the restriction level. It is worth noting that the liquid flowing through the restriction exerts

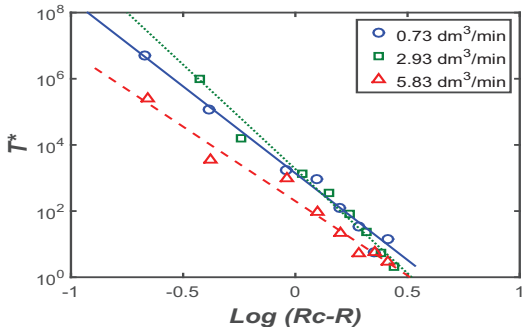

Figure 3. Power law divergence of avalanche size (spheres).

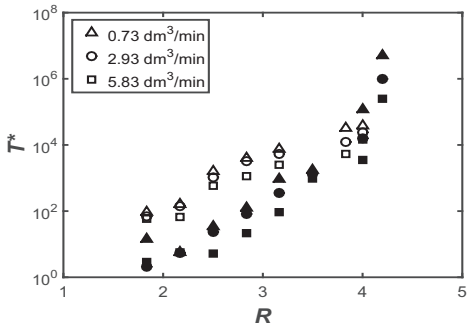

Figure 4. Avalanche size for spheres (filled) and polyhedra (empty).

a compressive stress on the granular assembly. Because of the high confinement ($W/d_P \approx 23$) and the monodispersity of the PSD, this leads to a strong ordering, very much like crystallization. Although it makes the interpretation of the results more complicated, this feature would have more degrees of freedom and the granular phase would experience the jamming later, on a statistically smoother basis. In this section, we study the influence of the restriction size, the liquid flow rate and the particle morphology on the avalanche size. We define the dimensionless opening ratio R as the restriction width w divided by the particle diameter d_P. It ranges between 1.83 and 4.2. The restriction cross-section area is labeled $\Sigma_r \equiv w.H = R.d_P.H$. Three flowrates Q_f are investigated: 0.73, 2.93 and 5.86 $dm^3.min^{-1}$. The particle morphology is characterized by the aspect ratio, which is 1 for spheres and 0.75 ± 0.05 for polyhedra. When the system is jammed, it forms a porous medium and the flow regime can be characterized by the Reynolds number $Re \equiv \rho_f.(Q_f/\Sigma).d_P/\mu_f$. In the channel upstream of the restriction, we have $\Sigma = \Sigma_c$ and the Reynolds number is equal to 70, 279 and 558 for the three different flow rates respectively. When approaching the arch, the fluid velocity increases and thus the Reynolds number. As an example, for the average values of $Q_f = 2.93$ $dm^3.min^{-1}$ and $R = 3$, its value is 2170 at the arch level ($\Sigma = \Sigma_r$). During an avalanche, the particles are entrained by the fluid and the slip velocity is reduced, presumably by a factor of the order of 1 to 10. All considered, our experimental conditions are characterized by a Reynolds number ranging between a few tens and a few hundred. According to Clift and Weber's terminology [10], it seems therefore reasonable to depicts the flow as weakly turbulent.

Experimental results show that the density probability decays exponentially with the avalanche size *i.e.*, the probability to have an avalanche of size T is proportional to $exp(-T/T^*)$, where T^* is a characteristic avalanche size. This is the signature of a Poisson process, characterized by the absence of memory effect. In our case, according to [9], the prevailing mechanism is the multi-bridging: when the local concentration is high enough right upstream the orifice, particles may try to simultaneously flow and instantaneously form a bridge. A strong analogy appears with the self-filtration phenomenon reported by Haw [11] for colloidal particles. Indeed, since the granular phase experiences more difficulties (collision, friction) to flow through the restriction than the liquid phase (which flowrate is imposed), the solid phase concentration is reduced upon crossing the restriction. This effect is obviously more pronounced in our experiment, where the dynamic arches are composed of a maximum of 5 to 10 grains. It would certainly deserve a more quantitative analysis. Whatever the liquid flowrate and the particle shape, experiments show that the characteristic avalanche size T^* gets very large when R is approaching a critical dimensionless opening ratio R_c. This divergence is also observed in classical thermodynamic phase transitions and thus suggests that it can be represented by a power law:

$$T^* = A.(R_c - R)^{-\gamma} \quad (1)$$

where A is a constant and γ an exponent characterizing the divergence speed. To determine these parameters, the least squares method is used. Fig. 3 confirms that this law interpolates the experimental results with a very good agreement for spheres. The agreement is good for polyhedra as well, though a little bit more scattered. The results are summarized in Tab. 1, which gives the values of A, R_c and γ for the three flow rates Q_f investigated in our work.

Table 1. Divergence parameters.

	Spheres			Polyhedra		
Q_f	A	R_c	γ	A	R_c	γ
0.73	1.4×10^3	4.4	5.3	1.4×10^7	5.9	7.9
2.93	1.9×10^3	4.6	6.3	1.9×10^5	5.6	6.3
5.86	2.0×10^2	4.4	4.5	2.0×10^6	5.9	6.8

4 Discussion

Tab. 2 compares the divergence velocity γ and the critical ratio R_c obtained in our work to the values given by Garcimartin [12], Thomas [13] and Lafond [14]. Whatever the system dimension (2D or 3D), the particle morphology (spheres or polyhedra), the driving force (viscous drag or gravity), the suspending fluid (gas or liquid), and the flow

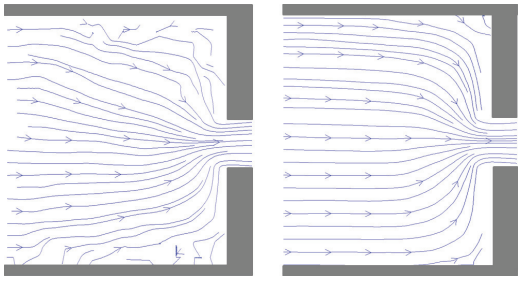

Figure 5. Particles streamlines for polyhedra (left) and spheres (right). Q_f =2.93 dm^3.min^{-1} and R =3.83.

Table 2. Comparison with the literature.

Authors	Particles	Fluid	Geometry	R_c	γ
This work	PE spheres 5.92 mm	Water Glycerol	≈ 2D Hor Visc. driven	4.5	5.35
This work	PE polyhedra 5-7 mm	Water Glycerol	≈ 2D Hor Visc. driven	5.8	7
Lafond	PS spheres 10-16 mm	Water Nacl	3D Horiz Visc. driven	3.6	
Garci--martin	Glass spheres 0.42–3 mm	Air	2D Vertic Grav. driven	4.9	6.90
Thomas	Glass spheres 2 mm	Air	3D Vertic Grav. driven	4.7	5

direction (vertical or horizontal), we observe that the critical opening ratio R_c is 4.7±1.2 and the divergence velocity γ is 6.0±1.0. The relatively small dispersion of these parameters suggests that the mechanisms underlying the flowing/jamming transition share some important properties, that still need to be resolved. Despite the similarities, small but significant differences can be highlighted. Here, we restrain our discussion to the influence of the particle morphology for moderate opening ratios. The velocity fields of the solid phase exhibit two regions: a central flow region (particle velocity up to 18 cm.s^{-1}) and a lateral dead zone, where particles are at rest (velocity below 2 mm.s^{-1}). For spheres, the dead zone is limited to a small region upstream of the restriction. In contrast, for polyhedra, the dead zone extends further upstream and laterally. Fig. 4 compares the characteristic avalanche size for spheres and polyhedra. Experimental results clearly demonstrate that, for opening ratios R below 3.5, avalanches of polyhedra are larger than avalanches of spheres by at least one order of magnitude !

We propose the following explanation for this apparent paradox. At the particle scale, the angular shape of polyhedra prevents them from rolling around each other. This strong reduction of the rotational degree of freedom leads polyhedra to form larger dead zones than spheres. At the system scale, the size and shape of the dead zones dictates the size and shape of the zone, where unjammed particles keep flowing. More precisely, as suggested by Fig.5, a large dead zone is associated with a gently converging flow, whereas a vanishingly small dead zone is associated with an abrupt change of the streamlines direction when approaching the restriction. In the second configuration, the probability of head-on collisions is thought to be significantly increased and explain the greater jamming probability. To test this hypothesis, we calculate the fraction of particles converging to the restriction with an angle θ to the main flow direction. As expected, Fig.6 shows that the frequency of a head-on collision is larger for spheres (abruptly converging flow) than for polyhedra (smoothly converging flow). As a perspective, it would be interesting to use liquids with different viscosities in order to investigate the complex role of the fluid, which acts as a driving force but also as a lubricant through the film drainage.

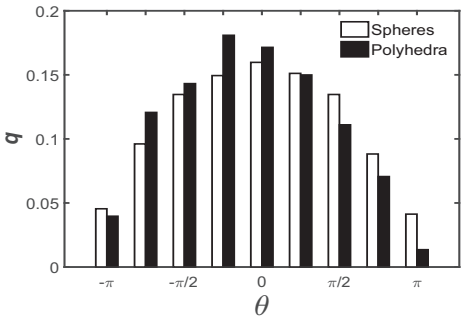

Figure 6. Normalized particle flow rate converging with angle θ towards the restriction center.

References

[1] K. To, Modern Physics Letters B **19**, 1751 (2005)
[2] I. Zuriguel, A. Garcimartín, D. Maza, L.A. Pugnaloni, J. Pastor, Phys Rev E **71**, 051303 (2005)
[3] A. Garcimartín, I. Zuriguel, D. Maza, J. Pastor, L. Pugnaloni, Experimental Chaos **742**, 279 (2004)
[4] A. Janda, I. Zuriguel, L. Pugnaloni, D. Maza et al., EPL **84**, 44002 (2008)
[5] T. Wilson, C. Pfeifer, N. Mesyngier, D. Durian, Papers in physics **6**, 060009 (2014)
[6] A. Guariguata, M.A. Pascall, M.W. Gilmer, A.K. Sum, E.D. Sloan, C.A. Koh, D.T. Wu, Phys Rev E **86**, 061311 (2012)
[7] P.G. Lafond, M.W. Gilmer, C.A. Koh, E.D. Sloan, D.T. Wu, A.K. Sum, Phys Rev E **87**, 042204 (2013)
[8] W. Beverloo, H. Leniger, J. Van de Velde, Chemical engineering science **15**, 260 (1961)
[9] M.M. Sharma, H. Chamoun, D.S.R. Sarma, R.S. Schechter, J. of colloid and interface science **149**, 121 (1992)
[10] R. Clift, J. Grace, M. Weber, Academic, New York pp. 171–202 (1978)
[11] M. Haw, Physical review letters **92**, 185506 (2004)
[12] A. Garcimartín, C. Mankoc, A. Janda, R. Arévalo, J.M. Pastor, I. Zuriguel, D. Maza, in *Traffic and Granular Flow'07* (Springer, 2009), pp. 471–486
[13] C. Thomas, D.J. Durian, PhysRev E **87**, 052201 (2013)
[14] P.G. Lafond, Ph.D. thesis, Colorado School of Mines. Arthur Lakes Library (2007)